

Article

Revealing the Molecular Interaction between CTL Base Oil and Additives and Its Application in the Development of Gasoline Engine Oil

Chunfeng Zhang¹, Xiaojun Zhang¹, Qiang Yan¹, Liyang Wang¹ and Xiangqiong Zeng^{2,*} 

¹ Shanxi Lu'an Taihang Lubrication Technology Co., Ltd., Changzhi 046200, China; zcf224@126.com (C.Z.); zhxjuna3051@yeah.net (X.Z.); 18830063716@163.com (Q.Y.); 15103454013@163.com (L.W.)

² School of Materials and Chemistry, University of Shanghai for Science and Technology, Shanghai 200093, China

* Correspondence: zengxq202312@163.com

Abstract: In order to improve fuel economy to meet the standard for passenger car oil, a new formulation with good viscosity–temperature performance for gasoline engine oil is required. In this study, coal-to-liquid (CTL) base oil, with a high viscosity index and good low-temperature performance, was selected as the base oil to develop the gasoline engine oil. A systematic study on the molecular interaction between the CTL base oil and the viscosity index improver (VII), including three kinds of hydrogenated styrene diene copolymers (HSD-type) and four kinds of ethylene propylene copolymers (OCP-type), was conducted. It was found that in general, in CTL base oil, the HSD-type VII exhibited a much higher viscosity index, a significantly lower shear stability index, a higher thickening ability, and a lower cold-cranking simulator (CCS) viscosity than that of OCP-type VII. Moreover, when comparing CTL base oil with mineral oil 150N, the combination of CTL base oil and the VII displayed a lower CCS viscosity than that of mineral oil, suggesting it had better low-temperature performance and was able to quickly form a protective oil film on the surface, which was beneficial for the cold start. The functional group distribution state of the VII in base oil was analyzed using synchrotron radiation micro-infrared microscope (SR Micro-IR) technology, which revealed that HSD-1 had a better molecular interaction with CTL6 than 150N because of the better uniformity of the C=C group distribution. Based on this, a SP 0W-20 gasoline engine oil was developed by the combination of CTL base oil and the HSD-1 viscosity index improver, together with an additive package, a polymethacrylate pour point depressant, and a non-silicone defoamer, which showed excellent low-temperature performance, thermal oxidation stability, and detergency performance compared to the reference oil.

Keywords: coal-to-liquid base oil; viscosity index improver; molecular interaction; gasoline engine oil



Citation: Zhang, C.; Zhang, X.; Yan, Q.; Wang, L.; Zeng, X. Revealing the Molecular Interaction between CTL Base Oil and Additives and Its Application in the Development of Gasoline Engine Oil. *Lubricants* **2024**, *12*, 275. <https://doi.org/10.3390/lubricants12080275>

Received: 8 May 2024

Revised: 12 June 2024

Accepted: 14 June 2024

Published: 31 July 2024



Copyright: © 2024 by the authors. Licensee MDPI, Basel, Switzerland. This article is an open access article distributed under the terms and conditions of the Creative Commons Attribution (CC BY) license (<https://creativecommons.org/licenses/by/4.0/>).

1. Introduction

With the increasingly stringent emission standards for automobiles and the continuous progress of engine technology, automotive lubricants are required to be developed towards energy conservation, environmental protection, economy, and high-quality levels [1,2]. In particular, the implementation of the passenger car oil standard GF-6B [3] has put forward higher requirements for automotive fuel economy. By using new formulation technologies to reduce viscosity and optimize anti-friction performance of gasoline engine oil, the lubrication and protection of engine oil for the engine can be improved, which is an effective way to improve fuel economy [4,5].

Base oil, as the main component of the lubricant formulation, affects the whole performance and service life of gasoline engine oil, like evaporation loss, pour point, viscosity index, oxidation stability, etc. For instance, due to the requirements of low-viscosity gasoline engine oil, a high-quality base oil with a low viscosity, high viscosity index (VI), and

low evaporation loss is preferred [6]. In addition, Kallas M. M. et al. studied the effect of synthetic, semi-synthetic, and mineral base oil of SAE10W40 engine oil on gasoline engine parts wear, and found that synthetic oil showed better performance than semi-synthetic and mineral oil [7].

With the progress in coal catalytic conversion technology and emission reduction technology, coal-to-liquid (CTL) base oil, obtained from coal gasification and then the Fischer–Tropsch catalytic reaction, shows the advantages of a high liquid recovery, low emissions, and cost effectiveness, especially for those countries with coal as the primary raw material [8–11]. Because the structure of CTL base oil is mainly alkanes with a high cetane number and low sulfur, nitrogen, and aromatic content, and the content of isomeric alkanes is much higher than normal alkanes, CTL base oil has a high VI and a low pour point, which makes it a high-quality and clean alternative fuel that can be used to formulate engine oil, compressor oil, hydraulic oil, gear oil, grease, etc. [12,13]. Moreover, CTL can be blended in any ratio with conventional petroleum-based fuels, so it is compatible with the existing automotive technology systems and has promising prospects for synthetic high-grade lube oil [14].

To provide guidance for the application of CTL base oil in the high-grade lube oil market, Yu X. et al. [12] examined the effect of antioxidant additives on the thermal oxidative degradation of CTL base oil and found that diphenylamine (L57) and 2,6-di-*tert*-butyl-4-methylphenol (T501) can significantly improve the oxidation stability of CTL base oil by inhibiting the formation of carbonyl groups (C=O), with a reduction in the diffusion coefficient of the antioxidant in CTL base oil, the free volume of O₂ in the CTL base oil being reduced, and the antioxidation performance increased. Zhang C. et al. [15] studied the correlation between the molecular structure and viscosity index of CTL base oils. It was found that CTL base oils with a similar carbon number distribution exhibited narrower distillation ranges, lower boiling points, and higher distillation efficiencies than those of mineral base oil, and the average chain length, normal paraffins, and structure S₆₇ (6- or 7-methyl-substituted CTL branched structure) caused the CTL base oil to display a higher VI.

Due to the change in structure of CTL base oil compared to traditional base oil, traditional gasoline engine oil additives and/or additive packages will not be applicable to CTL base oil. Therefore, it is very important to explore the molecular interaction between CTL base oil and additives in order to develop CTL-based gasoline engine oil. For reducing viscosity and improving anti-friction performance of gasoline engine oil, various additives including lubrication additives, pour point depressants, viscosity index improvers, etc. were used [16–18]. Among these, the viscosity index improver (VII) is one of the key additives to optimize the viscosity–temperature performance of gasoline engine oil. It indicates the degree of change in viscosity as a function of temperature. A high VI means a small change in viscosity with the change in temperature, so the oil can be thin enough to easily start at low temperatures and remain thick enough to provide good lubrication at high temperatures [19]. Boussaid M. et al. [20] investigated the potential of using polyethylene glycol (PEG) as a VII to improve the VI of paraffinic oil. Polyethylene glycol 1500 was blended with 150NS at a concentration from 0 to 10%. It was found that the optimum performance was obtained for the blend containing 3% PEG, resulting in the highest VI of 114.67 due to good particle distribution, evidenced by a smaller polymer particle size and smaller activation energy difference. It was confirmed that the dispersion of the polymer in the oil was crucial for improving the VI, even in the absence of intermolecular interactions. Mohamad S.A. et al. [21] synthesized six polyacrylate copolymers with C8 to C16 alkyl-chain-length alcohols, and their viscosity-improving performance in base oil SAE 30 was studied under the concentration of 0.5–3%. The results showed that all of the prepared polyacrylate copolymers were effective as VIIs for lube oil, and their effectiveness became more pronounced with the increase in either the concentration, the molecular weight (140,000–236,000), or the alkyl chain length (C8–C12) of the copolymers. Similarly, Ghosh P. et al. [22] compared the VI-enhancing capability of decyl and isoctyl

acrylate polymers in two kinds of mineral base oils. The results suggested that the isoctyl acrylate polymer showed a higher VI and pour point depression efficiency than that of the decyl acrylate polymer, which depended on the nature of the mineral base oils as well as the type and concentration of the VIIs. Further, Lomège J. et al. [23] synthesized plant-oil-based amide copolymethacrylate as a VII in an organic triglyceride lube oil. It was found that the thickening power can be improved by increasing the copolymer molecular weight, concentration, dispersity, and pendant aliphatic chain length, or by adding an additional aliphatic chain in the copolymer backbone. In addition, polyvinyl palmitate copolymer has been investigated as a VII in diesel oil [24], MWCNT and ZnO nanoparticles have been studied as VIIs in 5W50 to improve engine oil lubrication in light-duty vehicles [25], a fatty-acid-based comb (co) poly(9-alkyl 12-hydroxystearate) was synthesized by click chemistry and studied as a VII in a mineral-based lubricant [26], and a core cross-linked star copolymer was synthesized and evaluated as a VII for application in hydraulic lubricants [27]. In addition, Khalafvandi et al. [28] studied the viscosity properties of three types of VIIs (ethylene propylene, star isoprene, and two di-block styrene isoprene) in different types of base oils (API Groups I, II, and III). It was found that intrinsic viscosity depended on the polymer molecular weight, and the size of the polymer depended on the solubility of the polymer in the base oil. Although various VIIs have been developed and their performances in different base oils have been evaluated, their suitability for use in CTL base oil has not been revealed yet.

Therefore, the aim of this study was to develop a kind of gasoline engine oil using new CTL base oil, based on the exploration of the interaction between the CTL base oil and one of the key additives, the VII. The interaction between the CTL base oil and two types of VIIs was investigated systematically, including three kinds of hydrogenated styrene diene copolymers (HSD-type) and four kinds of ethylene propylene copolymers (OCP-type). The functional group distribution state of the viscosity index improver in the CTL base oil was revealed using synchrotron radiation micro-infrared microscope technology. Based on this, a SP 0W-20 gasoline engine oil was developed, and its low-temperature performance, thermal oxidation stability, and detergency performance were evaluated. The reason for choosing SP 0W-20 as our target was its high market share and moreover, new engines are designed to use lower-viscosity oils to reduce friction losses, since it was found that lowering lube oil viscosity from 10W40 to 0W10 yields a 4% improvement in fuel economy [29].

2. Materials and Methods

2.1. Materials

The base oils used in this study included coal-to-liquid base oils (CTL4 and CTL6, both prepared through coal gasification and then the Fischer–Tropsch catalytic reaction by Shanxi Lu'an company, and the distribution of carbon number of CTL4 and CTL6 is shown in Table S1), Ketjenlube 15 (KL15, dibasic acid ester, supplied by Italmatch Chemicals), and 150N (supplied by Formosa Plastics Group, and the distribution of the carbon number of 150N is shown in Table S1 as well). Their physical and chemical properties are displayed in Table 1, and the test equipment and method for each test are listed in Table S2. The additives used included an additive package (AP, supplied by Afton) with dark brown color, density of 0.935 g/mL at 15 °C, flash point of at least 175 °C, kinematic viscosity of 173 mm²/s at 100 °C, total base number of 62 mg KOH/g, and element contents of P (0.57 wt.%), Ca (0.99 wt.%), Zn (0.65 wt.%), N (0.96 wt.%), Mg (0.33 wt.%), and Mo (0.03 wt.%), a polymethacrylate pour point depressant (PPD) with a kinematic viscosity of 189.6 mm²/s at 100 °C, and a non-silicone defoamer (DF) with a kinematic viscosity of 8.548 mm²/s at 100 °C. The viscosity index improvers we studied included three kinds of hydrogenated styrene diene copolymers (HSD-1, HSD-2, and HSD-3) and four kinds of ethylene propylene copolymers (OCP-1, OCP-2, OCP-3, and OCP-4). Their code and supplier information is listed in Table S3. Their physical and chemical properties were evaluated and analyzed, as shown in Sections 2.3 and 3.1.

Table 1. The physical and chemical properties of the base oils used.

Name	Kinematic Viscosity (100 °C, mm ² /s)	Kinematic Viscosity (40 °C, mm ² /s)	Viscosity Index	CCS Viscosity (−30 °C, mPa·s)	Pour Point (°C)	Flash Point by Open Cup (°C)	Evaporation Loss (NOACK, 250 °C, 1 h, %)
CTL4	4.155	17.80	141	922	−33	210	11.3
CTL6	6.181	31.34	150	2497	−36	247	3.9
KL15	5.350	27.00	138	4151	−63	235	7.5
150N	5.258	29.17	112	4483	−24	229	12.4

2.2. Preparation of the Base Oil and Viscosity Index Improver Blends

To study the interaction between viscosity index improver and the base oil, the base oil was blended with the viscosity index improver to make sols, and their solubility and stability, thickening ability, various kinematic viscosity, cold-cranking simulator viscosity index, and shear stability index were evaluated and analyzed.

The blends were made as follows: Firstly, 88 g of base oil was placed in a beaker and heated to 85 ± 5 °C. Then, under stir, 12 g viscosity index improver (VII solid) was slowly added to the base oil (in a ratio of 12 wt.% VII: 88 wt.% base oil) and heated to 135 °C. The solution was stirred at 135 °C for at least 8 h until the viscosity index improver dissolved completely. Stirring was stopped and the solution was maintained at 110 °C for another 8 h, then cooled down to obtain the liquid samples (VII liquid). The liquid sample was mixed with the base oil in a ratio of 1:9 (VII liquid : base oil) to obtain the sol samples (VII sol). The base oil used included CTL6 and 150N, respectively.

2.3. The Characterization of the Viscosity Index Improver Blends

2.3.1. The Solubility Test

The solubility of the VIIs in the base oils were tested by observing the appearance of the blends (VII sols) after storing at different temperatures (0 °C, −10 °C, −20 °C, −30 °C, and −40 °C) for 2 h, one after the other, and then recovering back to room temperature (rt.).

2.3.2. The Physico-Chemical Property Measurements

The physico-chemical properties of the VII blends (VII sols) were measured according to standard methods, including the kinematic viscosity (40 °C, 100 °C, mm²/s), VI, cold-cranking simulator viscosity (CCS, −20 °C, mPa·s), kinematic viscosity after shearing (100 °C, mm²/s), thickening ability (mm²/s), and shear stability index (SSI). The test equipment and method for each test are listed in Table S2. The thickening ability was calculated based on the kinematic viscosity at 100 °C according to SH/T 0622 with the following equation.

$$T = \nu_t - \nu_b$$

Here, T is the thickening ability (mm²/s), ν_t is the kinematic viscosity of the base oil with the viscosity index improver at 100 °C (mm²/s), and ν_b is the kinematic viscosity of the base oil at 100 °C (mm²/s).

In addition, the one-way ANOVA test and multiple t-test were used to conduct the statistical analysis. In the figures in Section 3, one asterisk (*) indicates significance at $p < 0.05$, and two asterisks (**) indicate significance at $p < 0.01$.

2.3.3. The Synchrotron Radiation Micro-Infrared Test

Synchrotron radiation micro-infrared test is a useful technique to illustrate the chemical group distribution of molecules. In this study, we applied the synchrotron radiation micro-infrared (SR Micro-IR) at BL01B beamline in Shanghai Synchrotron Radiation Facility (SSRF) to analyze the chemical group distribution of the VII in the base oil.

2.4. Preparation of the Gasoline Engine Oil

The SP 0W-20 gasoline engine oil developed in this work was prepared as follows: The base oil (CTL4, CTL6, KL15) was added to the reaction kettle, then stirred and heated to 60 °C. Then, the additive VII liquid (12 wt.% VII mixed with 88 wt.% CTL6, as described in Section 2.2), AP, PPD, and DF was added to the base oil in turn. The temperature was maintained at 60 °C while stirring for 2 h, then cooled down while stirring to obtain the SP 0W-20 gasoline engine oil samples.

2.5. The Physico-Chemical Property Measurements of the Developed Gasoline Engine Oil

The physico-chemical properties of the developed gasoline engine oil were measured according to standard methods, including the kinematic viscosity (100 °C, mm²/s), VI, low-temperature dynamic viscosity (−35 °C, mPa·s), low-temperature pumping viscosity (−40 °C, mPa·s), high temperature and high shear viscosity (150 °C, mPa·s), evaporation loss (%) and foam property (ml/mL), pour point, flash point, etc. The test equipment and method for each test are listed in Table S2.

2.6. The Performance Evaluation of the Developed Gasoline Engine Oil

2.6.1. The Thermal Oxidation Stability Test

The thermal oxidation stability of the developed gasoline engine oil was tested by Crankcase Simulation test to simulate the lacquer and coking formation of the oil during piston working, according to SH/T 0300, similar to FTM 791-3462, using internal combustion engine oil coking tendency tester C-9 supplied by Shanghai Rundi Scientific Instrument Co., Ltd. (Shanghai, China). The tested oil sample was sprayed onto an aluminum sheet at a high temperature, and due to the oxidation of the oil, a coking film was formed on the sheet. During the test, the oil samples and aluminum plate were maintained at 150 °C and 320 °C, respectively, in the Crankcase simulation tester, and operated for 6 h. After this, the color and scale level of the lacquer and coking film were assessed on a 1-to-10 scale according to the reference card, and the coking film weight on the aluminum plate was evaluated, which was correlated to the thermal oxidation stability of the oil [30].

2.6.2. The Detergency Test

The detergency of the developed gasoline engine oil was tested by the hot tube method according to SH/T 0645, using a hot tube tester R1091G supplied by Shanghai Rundi Scientific Instrument Co., Ltd. The oil sample and oxygen were mixed together and circulation refluxed in hot tube at 275 °C for 4 h. Then, the deposits generated in the glass tube were assessed by ranking the color and length of the formed lacquer on a scale of 0 to 10 according to the reference card, which was correlated to the detergency of the test oil [30].

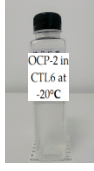
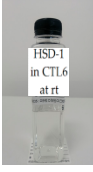


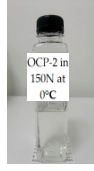
3. Results and Discussion

3.1. The Interaction between the Viscosity Index Improver and the Base Oil

3.1.1. The Solubility Analysis

The VII and the base oil were blended together to make sols as described in Section 2.2. The appearance of the blends (VII sols) under different temperatures was evaluated and is exhibited in Table 2, in which the base oils used for the stability tests were CTL6 and 150N, respectively. From the images in Table 2, we can see that all the VIIs could be dispersed well in both base oils, with a transparent white to light yellow appearance after being stored at 0 °C and −10 °C for 2 h. When the storing temperature was reduced to −20 °C, the sols became translucent, while when the temperature increased to room temperature again, the sols turned transparent again, indicating the good solubility of the VIIs in both base oils.

Table 2. The appearance of the blends under different temperatures.

Base Oil	Temperature (°C)	HSD-1	HSD-2	HSD-3	OCP-1	OCP-2	OCP-3	OCP-4
CTL6	0							
	-10							
	-20							
	rt.							
150N	0							
	-10							
	-20							
	rt.							

3.1.2. The Influence of VII Concentration on the Viscosity of the Blends

The VII is used to optimize the viscosity–temperature performance. As demonstrated by Coutinho [19], the viscosity of a VII polymer solution depends on many factors, including the chain size of the VII polymer, the concentration, the nature of the base oil, the strength of the inter- and intra-molecular interactions among the VII polymer molecules, and the degree of the interaction between the VII polymer molecules and the base oil. Therefore, firstly we investigated the effect of the VII concentration on the viscosity of the blends (VII liquid). Here, the VII liquid was made by mixing the VII solid (HSD-1 and OCP-1, respectively) with the base oil (CTL6 and 150N, respectively) at concentrations of 0.5%, 1.0%, 1.5%, 2.0%, and 3.0% using the same method as described in Section 2.2.

The results are illustrated in Figure 1. It can be found that no matter which VII and base oils used, with the increase in VII concentration, the kinematic viscosity at both 40 °C (Figure 1a) and 100 °C (Figure 1b), and the viscosity index (Figure 1c) were all increased.

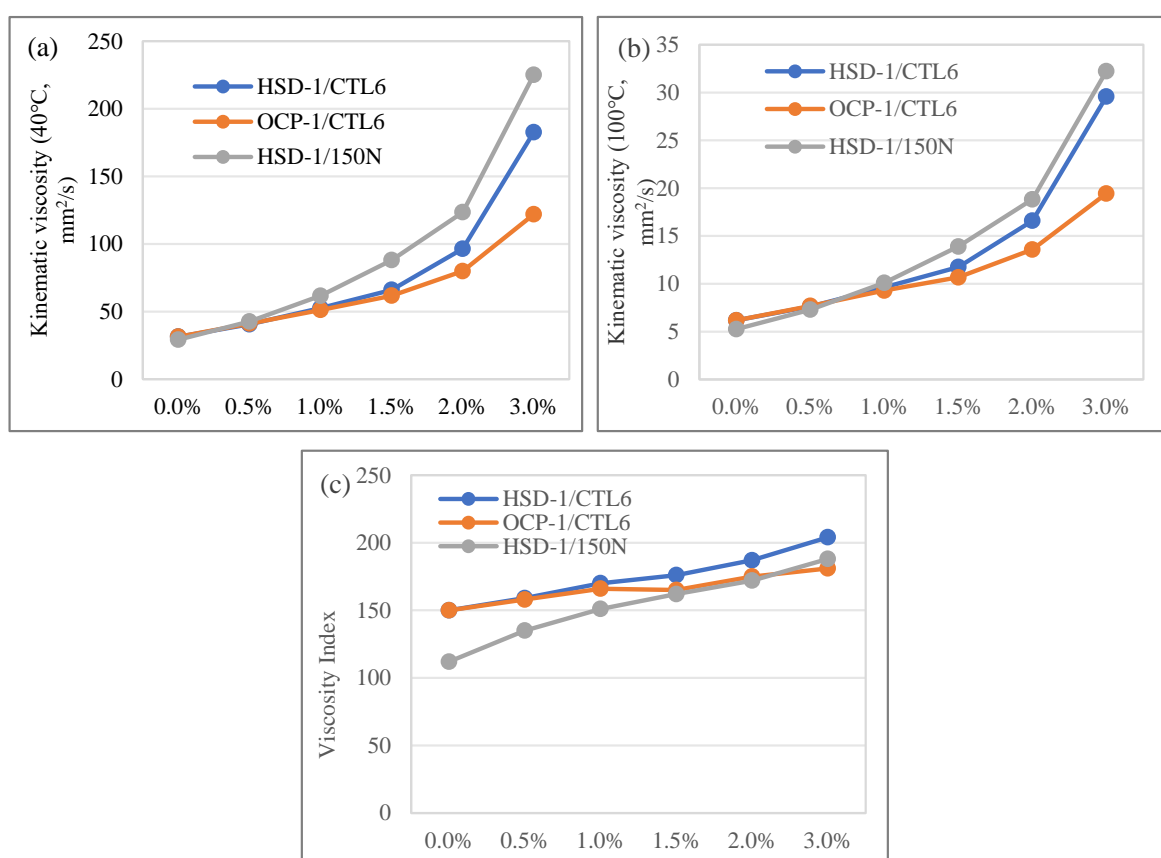


Figure 1. The influence of VII concentration on the viscosity of the blends: (a) Kinematic viscosity at 40 °C; (b) Kinematic viscosity at 100 °C; (c) Viscosity index.

When comparing the HSD-type VII (HSD-1) with the OCP-type VII (OCP-1) in CTL6, it can be seen that the kinematic viscosity of HSD-1 was higher than that of OCP-1 at both 40 °C and 100 °C, and the viscosity index of HSD-1 was higher than that of OCP-1, indicating HSD-1 had a smaller change in viscosity with the change in temperature than that of OCP-1 in the CTL6 base oil.

When comparing HSD-1 in the CTL6 and 150N base oils, we found that the kinematic viscosity of HSD-1 in 150N was higher than that in the CTL6 base oil at both 40 °C and 100 °C, while the viscosity index of HSD-1 in 150N was smaller than that in the CTL6 base oil, indicating that when used in the 150N base oil, the HSD-1 has a higher change in viscosity with the change in temperature.

Therefore, it can be concluded that HSD-1 had better viscosity–temperature performance than that of OCP-1, and it had better performance in CTL6 than in 150N. Usually, as the temperature increased the extent of the intra- and intermolecular interactions of VII and base oil reduced [19]. The results suggested that CTL6 was a good solvent for the HSD-1-type VII due to its ‘pure’ hydrogenated polyisoprene block, while 150N was a poor solvent for the HSD-1-type VII. In the good solvent CTL6, HSD-1 (hydrogenated styrene diene copolymer) was well dispersed, with the polymer chains uncoiled. Therefore, as the temperature rose, the reduction in bond strength was consequently low, so that the viscosity index was high. In the poor solvent 150N, the temperature increase may have provoked the increase in hydrodynamic volume of the HSD-1 polymer molecules and hence an increase in viscosity and a decrease in viscosity index compared to that in CTL6 [19].

3.1.3. The Influence of Type of VII on the Shear Stability of the Blends

In an automotive engine, lubricants are subjected to mechanical shearing like engine running. If the shearing force is too strong to break some chemical bonds in the VII polymer, then its molecular weight will reduce, resulting in a loss in its efficiency, affecting the quality level and service life of gasoline engine oils [19]. Therefore, shear stability is an important property of a VII. According to the API standard, the shear stability index of gasoline engine oil should be no more than 35 for GF-6 vehicles.

Firstly, the kinematic viscosity of the blends (VII sols) before and after shearing was measured and is displayed in Figure 2a,b. The kinematic viscosity of all samples was reduced after shearing, and in general, the viscosity-reducing degree of the OCP-type VII was higher than that of the HSD-type VII. Also, this phenomenon was further confirmed by the shear stability index (SSI), as illustrated in Figure 2c. In addition, the statistical analysis indicated that there was a significant difference among different types of VIIs. For the kinematic viscosity at 100 °C before shearing, between HSD-1 and OCP-3, OCP-1 and OCP-2, and OCP-1 and OCP-4, there was no obvious difference in either CTL6 and 150N, HSD-2 and HSD-3 showed no obvious differences in CTL6, and OCP-2 and OCP-4 showed no obvious differences in 150N. For the kinematic viscosity at 100 °C after shearing, OCP-1 and OCP-2 showed no obvious differences in either CTL6 or 150N; additionally, OCP-1 and OCP-3, and OCP-2 and OCP-3 showed no obvious differences in 150N, and HSD-2 and HSD-3, OCP-1 and OCP-4, and OCP-2 and OCP-4 showed no obvious differences in CTL6. The results suggested that the behavior of OCP-1 from Arlanxco and OCP-2 from Shenzhen Kunvii Petrochemical Technology were almost similar with respect to kinematic viscosity at 100 °C before and after shearing in both CTL6 and 150N. The rest of the samples all had significant differences.

From Figure 1c, it can be seen that the SSI of the VII in 150N was higher than that in CTL6; there was an especially significant difference between 150N and CTL6 for OCP-1 ($p < 0.05$), OCP-3 ($p < 0.01$), and OCP-4 ($p < 0.05$), indicating that the CTL and VII blends showed better shear stability than the mineral oil and VII blends. Moreover, the statistical analysis found that the SSIs of all the HSD-type VIIs were significantly lower than those of all the OCP-type VIIs in both CTL6 and 150N. Especially, HSD-1 showed the lowest SSI of 2.30 in the CTL6 base oil and 2.95 in the 150N base oil, suggesting the better shear stability of the HSD-1-type VII in CTL6. Within the groups, HSD-2 and HSD-3, and OCP-1 and OCP-2 showed no obvious differences in either CTL6 or 150N, and OCP-4 showed no obvious differences between OCP-1 and OCP-2 in 150N. Therefore, it can be concluded that the HSD-type VII and CTL base oil blends were promising in the development of gasoline engine oil in terms of shear stability.

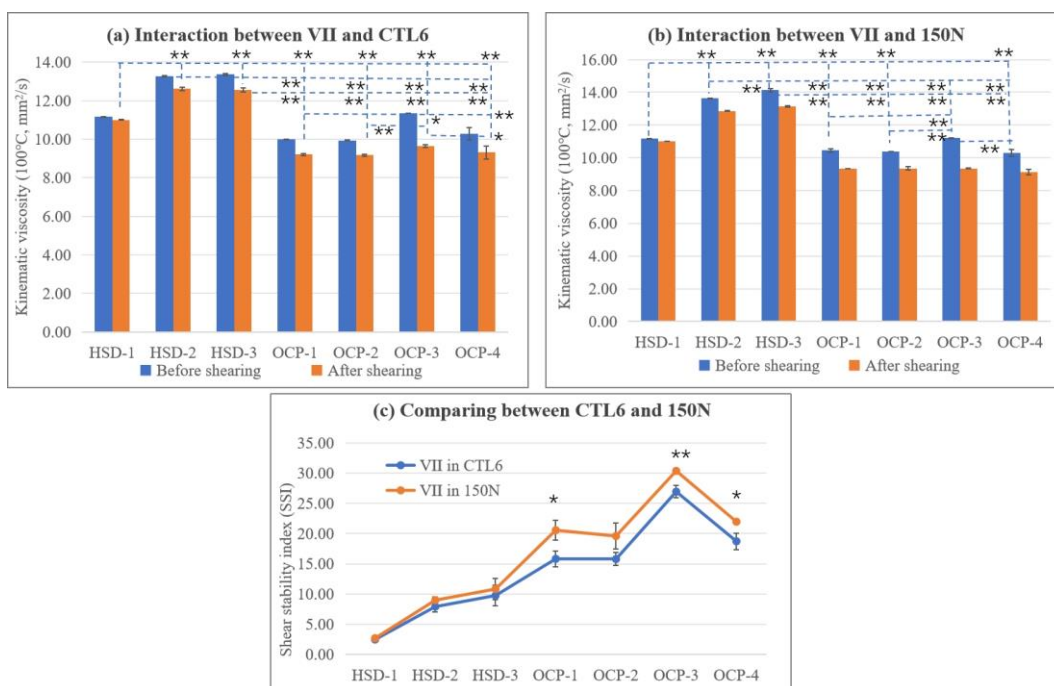


Figure 2. The shear stability of the VII and base oil blends: (a) Kinematic viscosity at 100 °C before and after shearing for VII in CTL6; (b) Kinematic viscosity at 100 °C before and after shearing for VII in 150N; (c) Shear stability index. (one asterisk (*) indicates significance at $p < 0.05$; two asterisks (**) indicate significance at $p < 0.01$).

3.1.4. The Influence of Type of VII on the Thickening Ability of the Blends

Thickening ability is another important parameter to evaluate the performance of a VII. Figure 3 exhibits the thickening ability of different types of VIIs in both CTL6 and 150N (VII sols). It can be seen that in general, the thickening ability of the VII in 150N was higher than that in CTL6, and there was significant a difference in thickening ability between 150N and CTL6 for HSD-2, HSD-3, OCP-1, and OCP-2.

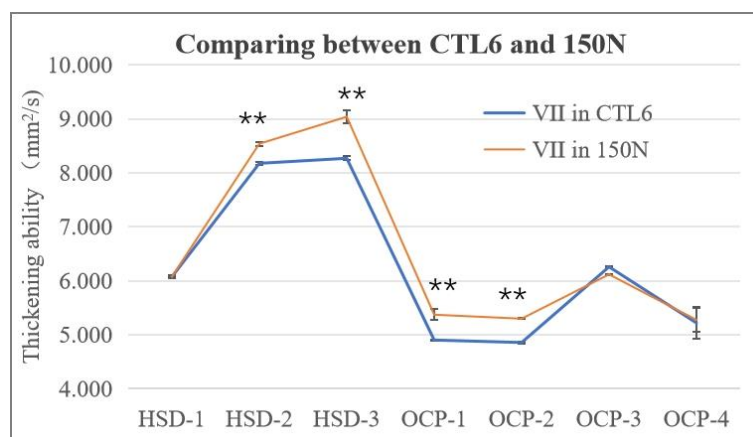


Figure 3. The thickening ability of the VII and base oil blends (two asterisks (**) indicate significance at $p < 0.01$).

In addition, no matter in which base oil, the HSD-type VII showed higher thickening ability than the OCP-type VII, and significant difference could be found between the HSD-type VII and the OCP-type VII, except for HSD-1 and OCP-3. Within the groups, there was no obvious difference between HSD-2 and HSD-3 in CTL6, between OCP-1 and OCP-2 in either CTL6 or 150N, between OCP-1 and OCP-4 in 150N, or between OCP-2 and OCP-4 in

150N. The rest of the samples all had significant differences. The better thickening ability of the HSD-type VII than the OCP-type VII may be due to the different networks formed. As a hydrogenated styrene diene copolymer, the HSD-type VII may form a polystyrene-block-associated network, while as an ethylene propylene copolymer, the OCP-type VII may form a moderately expanded dispersed network [19].

3.1.5. The Influence of Type of VII on the Low-Temperature Performance of the Blends

A VII can improve the viscosity–temperature performance of oil, but in the meantime, it may increase the low-temperature viscosity, affecting the cold start performance of the oil. Therefore, it is important to study the influence of VIIs on low-temperature performance.

Cold-cranking simulator viscosity (CCS, $-20\text{ }^{\circ}\text{C}$, mPa·s) is a parameter showing the torque necessary to turn the crankshaft in the lubricant, which is correlated to the cold start property. As can be seen in Figure 4 for the VII sols, no matter in which base oil, the CCS of the HSD-type VII was significantly lower than that of the OCP-type VII, except between HSD-1, HSD-3, and OCP-4. Moreover, no matter which VII was used, the CCS in the CTL6 base oil was lower than that in 150N, and there was a significant difference in the CCS between 150N and CTL6 for HSD-2, OCP-1, OCP-2, and OCP-3, suggesting that the CTL base oil with the addition of the HSD-type VII had the better low-temperature performance, with a better low-temperature fluidity beneficial for a cold start.

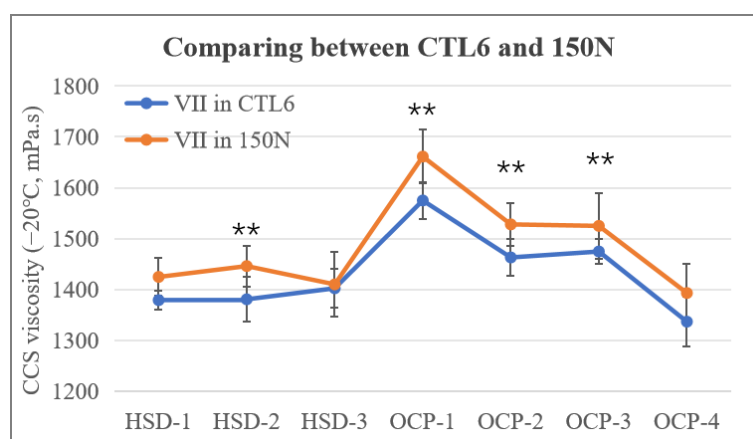


Figure 4. The low-temperature performance of the VII and base oil blends (two asterisks (**)) indicate significance at $p < 0.01$).

3.2. The Characterization of the Molecular Interaction between the Viscosity Index Improver and the Base Oil

To reveal the molecular interaction between the VII and base oil, Pirouz et al. [31] applied pyrene excimer fluorescence to quantitatively measure the molar fraction of the intermolecular interactions (f_{inter}) between ethylene propylene copolymers in toluene in the presence of wax, and Gholami et al. [32] used fluorescently labeled PPD to probe the interactions between PPD, VII, and wax in octane. In this study, the chemical group distribution of VII in base oil (VII sols) was analyzed using the synchrotron radiation micro-infrared (SR Micro-IR) technique.

The OCP-type VII is an ethylene propylene copolymer; therefore, it has the IR characteristic absorption peaks of the $-\text{CH}_2-$ chemical group at around 2915 cm^{-1} for the asymmetric stretching vibration, around 2846 cm^{-1} for the symmetric stretching vibration, and around 1459 cm^{-1} for the bending vibration. However, due to the similar IR characteristic absorption peaks of the OCP-type VII in both CTL and mineral oil, it is hard to analyze the distribution of the chemical group of the OCP-type VII in base oil. Meanwhile, the HSD-type VII is a hydrogenated styrene diene copolymer, which has the IR characteristic absorption peaks of the benzene ring skeleton ($\text{C}=\text{C}$) stretching vibration at around 1600 cm^{-1} and 1500 cm^{-1} . Therefore, it is valuable to analyze the chemical group

distribution of the HSD-type VII in base oils. Also, the test results of the C=C stretching vibration absorption peak (around 1490 cm^{-1}) distribution of the HSD-type VII in base oil are shown in Figure 5. It is obvious that in CTL6, the uniformity of the C=C group distribution was ranked as HSD-1 \approx HSD-2 > HSD-3, which was consistent with the performance of the HSD and base oil blends. In addition, the uniformity of the C=C group distribution in CTL6 (Figure 5(a2)) was much better than that in 150N (Figure 5(d2)), indicating a better molecular interaction for HSD-1/CTL6 than that for HSD-1/150N [33,34].

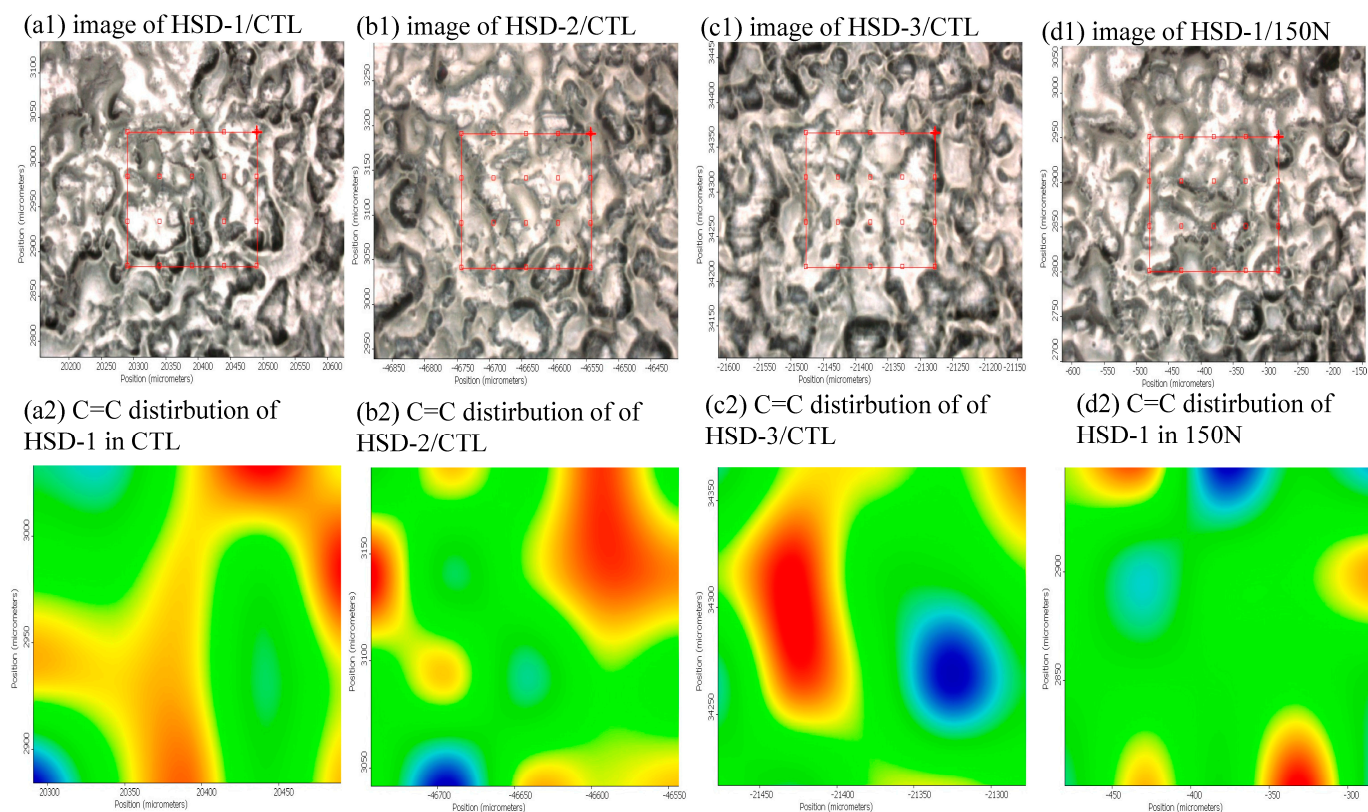


Figure 5. The chemical group distribution of HSD–type VII in base oils.

3.3. The Influence of the Concentration of the Viscosity Index Improver on the Physico-Chemical Properties of the Gasoline Engine Oil

Based on the study on the interaction between the VII and base oil, the HSD-1 VII was selected to develop the gasoline base oil. The formulation of the developed gasoline engine oil is displayed in Table 3, in which the concentration of the VII liquid and the ratio of the base oils were varied.

Table 3. The formulation of the developed gasoline engine oil.

Items	CTL4	CTL6	KL15	HSD-1 Liquid	AP	PPD	DF	In Total
F#1	62.59%	10.00%	10.00%	4.00%	13.10%	0.30%	0.01%	100.00%
F#2	64.59%	10.00%	10.00%	2.00%	13.10%	0.30%	0.01%	100.00%
F#3	12.00%	62.59%	10.00%	2.00%	13.10%	0.30%	0.01%	100.00%

Their physico-chemical properties compared to reference oil SP 0W-20 are exhibited in Table 4. Firstly, we compared F#2 and F#3 with the difference between the CTL4 and CTL6 base oil ratio, and it can be seen that although all the properties were within the qualification, the low-temperature dynamic viscosity of F#3 with a higher CTL6 ratio was

6100 mPa·s, approaching the upper limit of 6200 mPa·s, and was much higher than that of the reference SP 0W-20 oil (3381 mPa·s), indicating a risk to low-temperature performance. Therefore, we increased the ratio of the CTL4 base oil and compared the influence of VII concentration, using 2.00% VII for F#2 and 4.00% VII for F#1. It was found that with the increase in CTL4 ratio, the kinematic viscosity of the formulation reduced dramatically from 8.45 mm²/s to 6.60 mm²/s, and the high temperature and high shear viscosity reduced from 2.817 mPa·s to 2.519 mPa·s, even lower than the qualification. To solve this problem, we increased the concentration of the VII (F#1). Also, from the physico-chemical properties shown in Table 4, we can see that the viscosity characteristics at different conditions of F#1 were comparable to that of the reference oil SP 0W-20. Moreover, the pour point, flash point, evaporation loss, and foam properties of the developed gasoline engine oil F#1 were even better than that of the reference oil SP 0W-20, indicating a better low-temperature fluidity and cold start property, safety, and low oil consumption characteristics. Therefore, F#1 was chosen to be the final gasoline engine oil formulation.

Table 4. The physico-chemical properties of the developed gasoline engine oil.

Items	Qualification	F#1	F#2	F#3	Reference SP 0W-20	Test Method
Kinematic viscosity (100 °C, mm ² /s)	5.6–9.3	8.90	6.60	8.45	8.76	GB/T 265 [35]
Viscosity index	report	177	168	170	171	GB/T 1995 [36]
Pour point, °C	≤−40	−48	−45	−45	−51	GB/T 3535 [37]
Flash point (opening), °C	≥200	235	231	228	229	GB/T 3536 [38]
Low-temperature dynamic viscosity (−35 °C, mPa·s)	≤6200	4636	4530	6100	3381	GB/T 6538 [39]
Low-temperature pumping viscosity (−40 °C, mPa·s, no yield stress)	≤60,000	14,887	11,562	22,624	16,300	SH/T 0562 [40]
High temperature and high shear viscosity (150 °C, mPa·s)	≥2.6	2.800	2.519	2.817	2.611	SH/T 0703 [41]
Evaporation loss (%)	≤15	8.30	8.42	5.80	10.0	SH/T 0059 [42]
Foam property (ml/mL)						
Procedure I (24 °C)	≤10/0	0/0	0/0	0/0	0/0	GB/T 12579 [43]
Procedure II (93.5 °C)	≤50/0	10/0	10/0	15/0	20/0	
Procedure III (Last 24 °C)	≤10/0	0/0	0/0	0/0	0/0	



3.4. The Performance of the Developed Gasoline Engine Oil

During the use of gasoline engine oil, certain components with poor thermal stability in the oil will gradually be oxidized due to long-term exposure to high-temperature and high-shear environments. As the degree of oxidation becomes severe, the oxidation products will further react and condense, ultimately generating macro-molecular substances that are insoluble in oil, known as high-temperature deposits, which will significantly affect the performance of the gasoline engine oil. Therefore, the thermal oxidation stability and detergency performance related to the high-temperature deposits were evaluated for the developed gasoline engine oil F#1.

3.4.1. The Thermal Oxidation Stability

The thermal oxidation stability of the developed gasoline engine oil was tested using Crankcase Simulation test, and the results are shown in Table 5. It was obvious that the developed gasoline engine oil F#1 had better thermal oxidation stability than that of the reference oil SP 0W-20, with smaller amounts of black deposits, with a lighter and more even color.

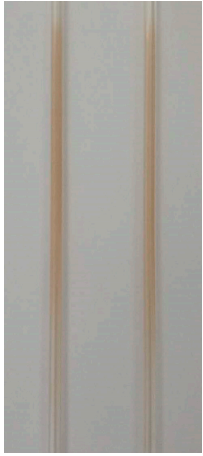

Table 5. The thermal oxidation stability of the developed gasoline engine oil.

Items	F#1	Reference SP 0W-20
Deposit weight (mg)	5	15
Color scale	1 + 1	3 + 0
Results description	Even, light yellow lacquer, carbon deposits level 1	Uneven bright patterns, carbon deposits level 2
Images of the plate surface		

3.4.2. The Detergency Performance

The detergency performance of the developed gasoline engine oil was tested using the hot tube test and the results are illustrated in Table 6. After the tests, both the developed gasoline engine oil and the reference oil SP 0W-20 showed a similar yellow lacquer with the color scale being the same at 6.5, suggesting the developed engine oil had similar detergency performance to that of the reference oil.

Table 6. The detergency performance of the developed gasoline engine oil.

Items	F#1	Reference SP 0W-20
Results description	Yellow lacquer	Yellow lacquer
Color scale	6.5	6.5
Images of the tube		

4. Conclusions

A gasoline engine oil SP 0W-20 was developed using CTL base oil and the HSD-type VII based on studying the interaction between the VII and base oil. The following conclusions can be drawn.

1. The interaction between three kinds of HSD-type VIIs, four kinds of OCP-type VIIs, and CTL and mineral base oils were systematically evaluated. It was found that firstly, all samples showed good solubility after storing at different temperatures. Secondly, no matter which VII and base oils were used, the kinematic viscosity and the viscosity index all increased with the increase in VII concentration. Also, the HSD-type VII illustrated a higher VI, smaller SSI, better thickening ability, and lower CCS viscosity than that of the OCP-type VII, and the HSD-type VII and CTL base oil combination exhibited the best shearing stability and low-temperature performance, which is promising for the development of gasoline engine oil.
2. The SR Micro-IR analysis revealed that HSD-1 had a better molecular interaction with CTL6 than 150N because of better uniformity of the C=C group distribution.
3. By adjusting the base oil ratio and VII concentration, a gasoline engine oil F#1 was developed, with comparable viscosity characteristics and detergency performance to that of the reference oil SP 0W-20, and with better low-temperature fluidity and cold start property, lower oil consumption characteristic and better thermal stability than that of the reference oil SP 0W-20.

Supplementary Materials: The following supporting information can be downloaded at: <https://www.mdpi.com/article/10.3390/lubricants12080275/s1>, Table S1: The chemical composition of the CTL base oils. Table S2: The equipment and test method information of all tests in the study. Table S3: The code and supplier information of VIIs used in the study.

Author Contributions: Methodology, X.Z. (Xiaojun Zhang); Validation, L.W.; Investigation, Q.Y.; Writing—original draft, C.Z.; Supervision, X.Z. (Xiangqiong Zeng). All authors have read and agreed to the published version of the manuscript.

Funding: This research received no external funding.

Data Availability Statement: The original contributions presented in the study are included in the article, further inquiries can be directed to the corresponding author.

Acknowledgments: We thank the BL01B beamline of the National Facility for Protein Science in Shanghai (NFPS) at Shanghai Synchrotron Radiation Facility, for the support in the synchrotron infrared micro-spectroscopy measurements (No. 2022-NFPS-PT-007342).

Conflicts of Interest: Authors Chunfeng Zhang, Xiaojun Zhang, Qiang Yan and Liyang Wang were employed by the company Shanxi Lu'an Taihang Lubrication Technology Co., Ltd. The remaining author declares that the research was conducted in the absence of any commercial or financial relationships that could be construed as a potential conflict of interest.

References

1. Tóth, Á.D.; Szabó, Á.I.; Leskó, M.Z.; Rohde-Brandenburger, J.; Kuti, R. Tribological properties of the nanoscale spherical Y₂O₃ particles as lubricant additives in automotive application. *Lubricants* **2022**, *10*, 28. [[CrossRef](#)]
2. Arumugam, S.; Ellappan, R.; Sriram, G. Degradation of engine components upon exposure to chemically modified vegetable oil-based automotive lubricant. *J. Indian Chem. Soc.* **2021**, *98*, 100227. [[CrossRef](#)]
3. *GF-6B:API 1509*; Engine Oil Licensing and Certification System. API Publishing Services: Washington, DC, USA, 2019.
4. Srivastava, G. Framework for brand positioning of automotive lubricants by using structural equation modelling. *Int. J. Manag. Pract.* **2023**, *16*, 89–103. [[CrossRef](#)]
5. Tóth, Á.D.; Knaup, J. Investigation of the tribological properties of nano-scaled ZrO₂ and CuO additive in automotive lubricants. *IOP Conf. Ser. Mater. Sci. Eng.* **2020**, *903*, 012015. [[CrossRef](#)]
6. Kang, G.; Zhang, F.; Liu, H.; Wei, B.; Jin, Z.; Lv, H. Rapid separation and API grades identification of base oil in low viscosity gasoline engine oil SN 0W-16. *ACS Omega* **2024**, *9*, 21270–21275. [[CrossRef](#)]
7. Kallas, M.M.; Al Sabek, M.S.; Saoud, Y. Experimental comparison of the effect of using synthetic, semi-synthetic, and mineral engine oil on gasoline engine parts wear. *Adv. Tribol.* **2024**, *2024*, 5997292. [[CrossRef](#)]

8. Tong, R.; Zhang, B.; Yang, X.; Wang, Y.; Zhang, L. A life cycle analysis comparing coal liquefaction techniques: A health-based assessment in China. *Sustain. Energy Technol. Assess.* **2021**, *44*, 101000. [[CrossRef](#)]
9. Zhang, Y.; Li, J.; Yang, X. Comprehensive competitiveness assessment of four coal-to-liquid routes and conventional oil refining route in China. *Energy* **2021**, *235*, 121442. [[CrossRef](#)]
10. Song, M.; Wang, Z.; Wang, W. An empirical study on technological innovation and corporate competitiveness of listed coal-to-liquids companies in China. *Front. Environ. Sci.* **2022**, *10*, 1043094. [[CrossRef](#)]
11. Kong, Z.; Dong, X.; Jiang, Q. Forecasting the development of China's coal-to-liquid industry under security, economic and environmental constraints. *Energy Econ.* **2019**, *80*, 253–266. [[CrossRef](#)]
12. Yu, X.; Zhang, C.; Wang, H.; Wang, W.; Jiang, C.; Peng, C.; Yang, K. Oxidation degradation analysis of antioxidant added to CTL base oils: Experiments and simulations. *J. Therm. Anal. Calorim.* **2023**, *148*, 7033–7046. [[CrossRef](#)]
13. Zhang, Z.; Zhang, C.; Cai, P.; Jing, Z.; Wen, J.; Li, Y.; Wang, H.; An, L.; Zhang, J. The potential of coal-to-liquid as an alternative fuel for diesel engines: A review. *J. Energy Inst.* **2023**, *109*, 101306. [[CrossRef](#)]
14. Sun, W.; Sun, Y.; Guo, L.; Zhang, H.; Yan, Y.; Zeng, W.; Lin, S. Comparative assessment of n-butanol addition in CTL on performance and exhaust emissions of a CI engine. *Fuel* **2021**, *303*, 121223. [[CrossRef](#)]
15. Zhang, C.; Wang, H.; Yu, X.; Peng, C.; Zhang, A.; Liang, X.; Yan, Y. Correlation between the molecular structure and viscosity index of CTL base oils based on ridge regression. *ACS Omega* **2022**, *7*, 18887–18896. [[CrossRef](#)]
16. Markandan, K.; Nagarajan, T.; Walvekar, R.; Chaudhary, V.; Khalid, M. Enhanced tribological behaviour of hybrid MoS₂@Ti₃C₂ MXene as an effective anti-Friction additive in gasoline engine oil. *Lubricants* **2023**, *11*, 47. [[CrossRef](#)]
17. Rahimi, B.; Semnani, A.; Nezamzadeh-Ejhieh, A.; Langeroodi, H.S.; Davood, M.H. Monitoring of the physical and chemical properties of a gasoline engine oil during its usage. *J. Anal. Methods Chem.* **2012**, *2012*, 819524. [[CrossRef](#)]
18. Kaleli, E.H.; Demirtas, S. Experimental investigation of the effect of tribological performance of reduced graphene oxide additive added into engine oil on gasoline engine wear. *Lubr. Sci.* **2023**, *35*, 118–143. [[CrossRef](#)]
19. Coutinho, F.M.B.; Teixeira, S.C.S. Polymers used as viscosity index improvers A comparative study. *Polym. Test.* **1993**, *12*, 415–422. [[CrossRef](#)]
20. Boussaid, M.; Haddadine, N.; Benmounah, A.; Dahal, J.; Bouslah, N.; Benaboura, A.; El-Shall, S. Viscosity-boosting effects of polymer additives in automotive lubricants. *Polym. Bull.* **2023**, *81*, 6995–7011. [[CrossRef](#)]
21. Mohamad, S.A.; Ahmed, N.S.; Hassanein, S.M.; Rashad, A.M. Investigation of polyacrylates copolymers as lube oil viscosity index improvers. *J. Pet. Sci. Eng.* **2012**, *100*, 173–177. [[CrossRef](#)]
22. Ghosh, P.; Das, M. Study of the influence of some polymeric additives as viscosity index improvers and pour point depressants-synthesis and characterization. *J. Pet. Sci. Eng.* **2014**, *119*, 79–84. [[CrossRef](#)]
23. Lomège, J.; Mohring, V.; Lapinte, V.; Negrel, C.; Robin, J.J.; Caillol, S. Synthesis of plant oil-based amide copolymethacrylates and their use as viscosity index improvers. *Eur. Polym. J.* **2018**, *109*, 435–446. [[CrossRef](#)]
24. Rathika, S.; Raghavan, P.S. Influence of polyvinyl palmitate copolymer as viscosity index improvers For lube. *Mater. Today Proc.* **2019**, *16*, 978–986. [[CrossRef](#)]
25. Esfea, M.H.; Aranib, A.A.A.; Esfandeh, S. Improving engine oil lubrication in light-duty vehicles by using of dispersing MWCNT and ZnO nanoparticles in 5W50 as viscosity index improvers (VII). *Appl. Therm. Eng.* **2018**, *143*, 493–506. [[CrossRef](#)]
26. Méheust, H.; Le Meins, J.-F.; Brûlet, A.; Sandre, O.; Grau, E.; Cramail, H. Fatty-acid based comb copolyesters as viscosity Index improvers in lubricants. *Eur. Polym. J.* **2022**, *181*, 111674. [[CrossRef](#)]
27. Sparnacci, K.; Frison, T.; Podda, E.; Antonioli, D.; Laus, M.; Notari, M.; Assanelli, G.; Atzeni, M.; Merlini, G.; Pó, R. Core-crosslinked star copolymers as viscosity index improvers for lubricants. *ACS Appl. Polym. Mater.* **2022**, *4*, 8722–8730. [[CrossRef](#)]
28. Khalafvandi, S.A.; Pazokian, M.A.; Fathollahi, E. The investigation of viscometric properties of the most reputable types of viscosity index improvers in different lubricant base oils: API groups I, II, and III. *Lubricants* **2022**, *10*, 6. [[CrossRef](#)]
29. Tseregounis, S.I.; McMillan, M.L.; Olree, R.M. Engine oil effects on fuel economy in GM vehicles-separation of viscosity and friction modifier effects. In *SAE Technical Paper Series-Fuel Economy and Wear Performance on Engine Oils*; Society of Automotive Engineers, Inc.: Warrendale, PA, USA, 1998; p. 982502.
30. Zhang, D.; Li, Z.; Wei, X.; Wang, L.; Xu, J.; Liu, Y. Study tribological properties of MoDTC and its interactions with metal detergents. *J. Tribol.* **2020**, *142*, 122201. [[CrossRef](#)]
31. Pirouz, S.; Duhamel, J. Using pyrene excimer fluorescence to probe the interactions between viscosity index improvers and waxes present in automotive oil. *Macromolecules* **2017**, *50*, 2467–2476. [[CrossRef](#)]
32. Gholami, K.; Frasca, F.; Duhamel, J. Probing the interactions between pour point depressants (PPDs), viscosity index improvers (VIIs), and wax in octane using fluorescently labeled PPDs. *Can. J. Chem.* **2022**, *100*, 688–696. [[CrossRef](#)]
33. Tan, L.; Huang, T.; Ma, J.; Li, J.; Song, Z.; Zhou, X.; Tang, Y.; Yang, L.; Zeng, X. Study on the effect of end group on the anti-corrosion behaviour of polyether derivatives. *J. Mol. Liq.* **2022**, *347*, 117991. [[CrossRef](#)]
34. Guo, Y.; Li, J.; Zhou, X.; Tang, Y.; Zeng, X. Formulation of lyotropic liquid crystal emulsion based on natural sucrose ester and its tribological behaviour as novel lubricant. *Friction* **2022**, *10*, 1879–1892. [[CrossRef](#)]
35. GB/T 265; Petroleum Products-Determination of Kinematic Viscosity and Calculation of Dynamic Viscosity. General Administration of Quality Supervision, Inspection and Quarantine of the People's Republic of China: Beijing, China, 1998.
36. GB/T 1995; Petroleum Products-Calculation of Viscosity Index. The State Bureau of Quality and Technical Supervision: Beijing, China, 1998.

37. *GB/T 3535*; Petroleum Products-Determination of Pour Point. General Administration of Quality Supervision, Inspection and Quarantine of the People's Republic of China: Beijing, China, 2006.
38. *GB/T 3536*; Petroleum Products-Determination of Flash and Fire Points-Cleveland Open Cup Method. General Administration of Quality Supervision, Inspection and Quarantine of the People's Republic of China: Beijing, China, 2008.
39. *GB/T 6538*; Determination of Apparent Viscosity of Engine Oils-Using the Cold-Cranking Simulator. The State Bureau of Quality and Technical Supervision: Beijing, China, 2022.
40. *SH/T 0562*; Standard Test Method for Determination of Yield Stress and Apparent Viscosity of Engine Oils at Low Temperature. National Energy Administration: Beijing, China, 2013.
41. *SH/T 0703*; Standard Test Method for Measuring Apparent Viscosity at High-Temperature and High-Shear Rate by Multicell Capillary Viscometer. National Energy Administration: Beijing, China, 2021.
42. *SH/T 0059*; Standard Test Method for Evaporation Loss of Lubricating Oils by the Noack Method. National Energy Administration: Beijing, China, 2011.
43. *GB/T 12579*; Determination of Foaming Characteristics of Lubricating Oils. General Administration of Quality Supervision, Inspection and Quarantine of the People's Republic of China: Beijing, China, 2002.

Disclaimer/Publisher's Note: The statements, opinions and data contained in all publications are solely those of the individual author(s) and contributor(s) and not of MDPI and/or the editor(s). MDPI and/or the editor(s) disclaim responsibility for any injury to people or property resulting from any ideas, methods, instructions or products referred to in the content.